Electromagnetic and Stress Analyses of the ITER Equatorial Thermal Shield

2013 Plasma Sci. Technol. 15 830

(http://iopscience.iop.org/1009-0630/15/8/22)

Electromagnetic and Stress Analyses of the ITER Equatorial Thermal Shield*

LEI Mingzhun (雷明准), SONG Yuntao (宋云涛), WANG Songke (王松可), WANG Xianwei (汪献伟)

Institute of Plasma Physics, Chinese Academy of Sciences, Hefei 230031, China

Abstract The ITER equatorial thermal shield is located inside the cryostat and outside the vacuum vessel, and its purpose is to provide a thermal shield from hot components to the superconducting magnets. Electromagnetic analysis of the equatorial thermal shield was performed using the ANSYS code, because electromagnetic load was one of the main loads. The 40° sector finite element model was established including the vacuum vessel, equatorial thermal shield, and superconducting magnets. The main purpose of this analysis was to investigate the eddy current and electromagnetic force in the equatorial thermal shield during plasma disruption. Stress analysis was implemented under the electromagnetic load. The results show that the equatorial thermal shield can accommodate the calculated electromagnetic loads.

Keywords: tokamak, thermal shield, finite element, electromagnetic analysis, ITER

PACS: *28.52.Av*

DOI: 10.1088/1009-0630/15/8/22

1 Introduction

The ITER equatorial thermal shield (ETS) is located outside the vacuum vessel (VV) and inside the cryostat. The function of the ETS is to minimize heat loads transferred by thermal radiation and conduction from warm components of the tokamak to the cool components of the superconducting magnets [1~8].

Due to complex working conditions, the ETS is subjected to different loads, such as gravity, seismic, electromagnetic (EM) and thermal gradients. In particular, very large eddy currents will be generated due to sudden changes of magnetic flux during plasma disruptions, and huge EM forces can be driven in the ETS structures. Therefore, transient EM analysis should be taken into account, and the EM load can be evaluated by further structural analysis [9].

2 Description of the equatorial thermal shield

The ETS consists of the vacuum vessel thermal shield (VVTS) and the equatorial cryostat thermal shield (ECTS), as shown in Fig. 1. The VVTS is interposed between the VV and the superconducting magnet structures. For space reasons, the VVTS has to closely follow the shape of the VV. The self-standing VVTS has 18 toroidal and 2 poloidal electrical breaks. The electrical insulation is formed by 2 mm thick fibreglass layer insulation between each flange and joint. A toroidal insulated joint is located between the VVTS inboard and outboard, and a poloidal insulated joint is located between the VVTS 20° sector and side 10° sector. The insulated joint can remarkably reduce eddy currents and corresponding EM forces, because electrical breaks lead to eddy current loops along the insulated joint. The VVTS is installed on the toroidal field coil. Two inboard and outboard supports are designated for each 20° VVTS sector. The inboard and outboard part of the VVTS is made of a thick plate with continuously welded flanges. Fig. 1 shows that the in-pit joint is located between the VVTS 40° sectors and a subassembly joint is used for connecting the VVTS 20° outboard sectors. There are two types of port joint, which are located between the outboard segment and the port thermal shield for connecting the port TS with the outboard panel. These joints do not have electrical breaks structure and have very little influence on induced currents. The ECTS is partially interposed between the VV ports and the magnet structures, but it predominantly covers and protects the superconducting magnet structures from heat radiating out from the cryostat [1,10,11].

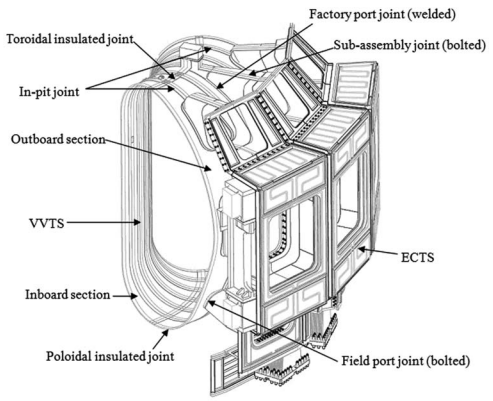

Fig.1 Location of the ETS

*supported by the International Thermonuclear Experimental Reactor (ITER) Specific Plan of China (No. 2009GB101004)

3 Electromagnetic analysis

A 3D transient EM analysis of the ETS was performed during plasma major disruption (MD) and vertical displacement events (VDE). Eddy current distribution and EM force distribution in the ETS structure were obtained for each load condition.

3.1 Analytical model

The 3D finite element model has been used to compute eddy current distribution and EM force distribution using the ANSYS commercial code. Because of the cyclic symmetry, the toroidal 40° sector model was established for the EM analysis based on CATIA data. All of conducting structure was built with Solid 97 elements, as well as the magnet coil, air and plasma volume. Infin 111 elements were used for the infinite boundary. The EM analysis model is composed of the VV, ETS, toroidal field (TF), poloidal field (PF), central solenoid (CS) coils and air. Hexagonal meshes were used for the VV, ETS, TF, PF, CS, and plasma volume, as shown in Fig. 2. 201658 elements and 69161 nodes were generated for EM analysis with a 40° sector.

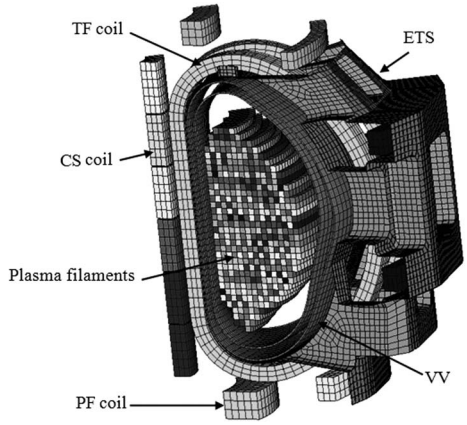

Fig.2 Finite element model of 40° sector for ETS EM analyses (the finite elements for air are not shown here)

3.2 Boundary and loading conditions

A cyclic symmetry boundary condition was implemented on both sides of the 40° sector, and three (A_x, A_y, and A_z) degrees of freedom (DOF) are coupled at both the planes cyclically. A volt DOF was also coupled in all conducting structures in the same way. An infinite boundary flag was applied to the infinite elements. All the nodes along the main axis of the ITER device were restrained by A_x, A_y, A_z DOFs, as shown in Fig. 3.

As to EM analysis for specified plasma events, the events to be considered were MD and the slow downward (SD) VDE. Three independent transient EM analyses have been performed for each case by considering two kinds of current quench. Case 1: plasma current exponential decays with a time constant of 22 ms, this event is expected to be a normal worst case. Case 2: plasma current exponentially decays with a time constant of 16 ms, this event is expected to be an upset worst case. Case 3: plasma slows downward vertical displacement event.

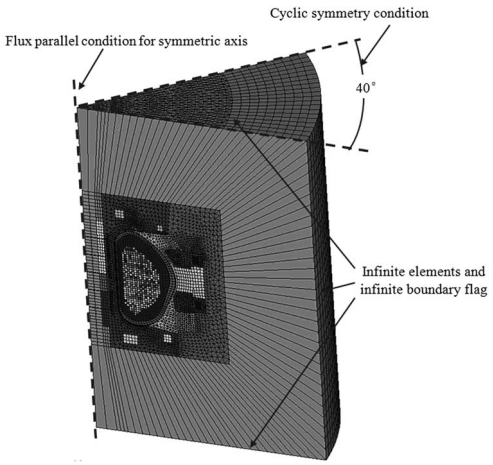

Fig.3 Boundary conditions for EM analyses

In this article, it is assumed that the current of the TF, PF, CS is constant, Because these magnets have very little influence on eddy current.

3.3 EM analysis results

The transient EM analyses have been performed to compute the eddy current density and EM force in the ETS induced by SD VDE and MD. Magnetic field distribution was also obtained. Table 1 lists the specification EM analysis results of the VVTS and ECTS under different plasma disruptions. It can be seen that the maximum eddy current density in ETS is primarily driven by the decay of the toroidal plasma current. The maximum value is 2.59E6 A/m^2, which occurs at 60 ms during the exponential decay with a time constant of 16 ms. It can also be seen that the maximum eddy current density in the exponential decay with time constant of 16 ms is a little greater than the value in the exponential decay with time constant of 22 ms. It arises from the fact that variations of magnetic flux in case 2 is a little faster than that in case 1. During SD VDE, eddy current and EM force are obviously smaller than other load cases. Fig. 4 shows the eddy current

Table 1. Main results of EM analyses

Load case	Maximum eddy current density (A/m^2)		Maximum node EM force (N)	
	VVTS	ECTS	VVTS	ECTS
Case 1	2.44E6	4.65E5	6501	135
Case 2	2.59E6	4.38E5	6894	128
Case 3	8.54E5	2.48E5	2438	104

distribution in ETS. The highest eddy current density is 2.59E6 A/m^2 at the central VVTS inboard at 60 ms. It is noticed that the main eddy current density is looped around the electrical insulation. The magnetic field distribution from all currents (including TF coils, PF coils, plasma, and the eddy current) was shown in Fig. 5, and the maximum magnet flux is 15.87 T at VVTS inboard regions. Fig. 6 shows the EM force acting on ETS generated by the coupling of induced eddy currents with the magnetic field. The peak value of EM force is 6894 N at 60 ms.

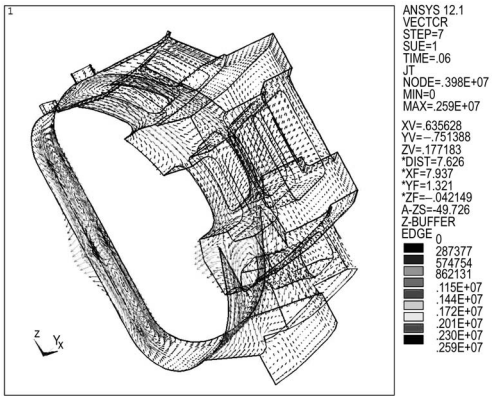

Fig.4 Eddy current density distribution for MD with 16 ms exponential current quenching at 60 ms (A/m^2)

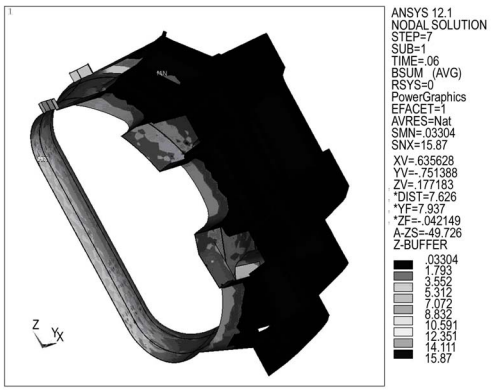

Fig.5 Magnetic field distribution for MD with 16 ms exponential current quenching at 60 ms (T)

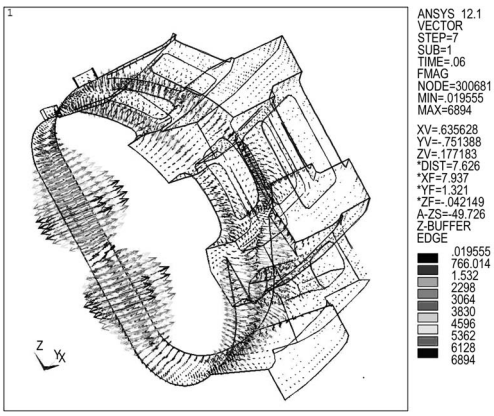

Fig.6 EM force distribution for MD with 16 ms exponential current quenching at 60 ms (N)

4 Structural analysis

4.1 Finite element model, boundary and loading conditions

A finite element model of the regular ETS part was established for structural analysis with Solid 45 elements. 7100 elements and 14662 nodes were generated for the analysis. The stress analyses were performed under deadweight and EM loads. The loads defined and boundary conditions for the analyses are as follows [12]. Fig. 7 shows the loading and boundary conditions for the EM load case.

Case 1: Deadweight

a. A symmetry boundary condition is applied, and all degrees of freedom of the inboard and outboard supports are fixed.

b. Gravity (vertical upward acceleration of 9.81 m/s^2).

Case 2: EM load

a. A symmetry boundary condition is applied, and all degree of freedoms of the inboard and outboard supports are fixed.

b. Gravity (vertical upward acceleration of 9.81 m/s^2).

c. EM load is applied as nodal force, which is obtained from transient EM analysis during plasma current exponential decays with a time constant of 16 ms.

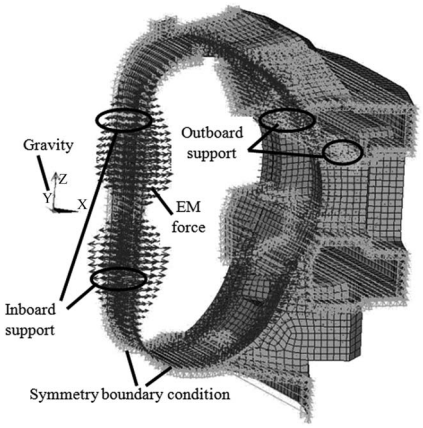

Fig.7 Loading and boundary conditions for analysis under EM load

4.2 Material properties and design criteria

The ETS is made of stainless 304L, 316LN, Inconel 718, titanium alloy (Ti-6Al-4V), and steel 660 [5]. The material properties of stainless 304L are summarized in Table 2. Since the mechanical properties of other materials are superior to stainless 304L at the same temperature, if the simulation results of the mechanical properties of stainless 304L can meet design requirements, we can confirm that the structure is reliable. ASME pressure vessel codes are used for the ETS design. Primary general bending stress (P_b) and membrane stress (P_m) resulting from gravity and the local membrane stress (P_L) resulting from the EM load are all primary

stresses [13]. According to the ETS design criteria, the requirement is as follows [3].

$$P_{\mathrm{m}} + P_{\mathrm{b}} < 1.5S_{\mathrm{m}} = 219 \text{ MPa}, \quad (1)$$

$$P_{\mathrm{L}} + P_{\mathrm{b}} < 1.5S_{\mathrm{m}} = 219 \text{ MPa}. \quad (2)$$

Table 2. Material properties of steel 304L

Temperature	Young's modulus	Poisson's ratio	Yield strength	Design stress intensity (S_{m})
80 K	209 GPa	0.3	219 MPa	146 MPa

4.3 Analysis result

This structure analysis aims at ensuring that the structure will not be damaged due to excessive deformations, stresses, and so on. The assessment requires comparison being made between the calculated results and the defined criteria. The structural analysis has been performed for the ETS under deadweight and EM load. Under the deadweight load, the maximum stress intensity of ETS is 26.8 MPa which occurs at the port region, and the maximum displacement is 0.92 mm. Fig. 8 illustrates the result of the stress intensity of the ETS under EM load. It can be seen that the maximum value is 150 MPa and locates at VVTS inboard. The maximum displacement is 2.23 mm, as shown in Fig. 8. Compared with the allowable stress, the results of the finite element analysis for the ETS show that the maximum stress is within allowable stress limits and thus the design requirements are satisfied.

Fig.8 Stress intensity (MPa) and displacements (m) of the ETS under EM load

5 Conclusion

In order to evaluate the EM loads in the ETS structure during plasma current disruption events, transient EM analyses have been performed using a 3D finite element model and the ANSYS computational code. Eddy current density distribution and EM forces were obtained. Comparison of the results obtained for three load cases suggests that the EM forces under plasma current exponential decays with time constant of 16 ms are larger than the other load cases. The maximum nodal force is 6894 N at 60 ms. Structural analyses have also been implemented for evaluating the ETS structure under deadweight and EM load. EM load is applied to the structural analysis model as nodal force for further analysis. The stress result shows that it is within the allowable designed stress limit. It has been proved that the present ETS design under deadweight and EM load is reasonable and feasible. These results will offer guidance for the design of the ETS. More detailed analysis should be done in the future.

Acknowledgment

The authors would like to express their sincere appreciation to all the members for excellent ITER TS design and analysis work at the ITER Site.

References

1 Hamlyn-Harris C, Her N I, Le Barbier R, et al. 2010, System Design Description (DDD) 27 Thermal Shield. ITER, 355MXD, France
2 Chung W, Kim B C, Sa J W, et al. 2008, Fusion Engineering and Design, 83: 1588
3 Her N I, Terasawa A, Yu J. 2010, Load Specification for the ITER Thermal Shields. ITER, 33N92A, France
4 Sonato P, Miki N, Testoni P, et al. 2002, Fusion Engineering and Design, 61∼62: 415
5 Liu Songlin, Long Pengcheng, Wang Weihua, et al. 2010, Fusion Engineering and Design, 83: 2176
6 Kotulski J D, Coats R S, Pasik M F. 2008, Fusion Engineering and Design, 83: 1068
7 Borovkov A, Gaev A, Nemov A, et al. 2007, Fusion Engineering and Design, 82: 1871
8 Panin Anatoly, Biel Wolfgang, Krasikov Yury, et al. 2011, Fusion Engineering and Design, 86: 2016
9 Kim Duck-Hoi, Oh Dong-Keun, Pak Sunil, et al. 2010, Fusion Engineering and Design, 85: 1747
10 Krasikov Yu, Bykov V, Dalle Carbonare G, et al. 2003, Fusion Engineering and Design, 66∼68: 1049
11 Bykov V, Krasikov Yu, Grigoriev S, et al. 2005, Fusion Engineering and Design, 75∼79: 155
12 Nam K, Her N I, Noh C H. 2010, Detailed Design of Thermal Shield. ITER, 34Z6V8, France
13 Xie Han, Liao Ziying. 2008, Plasma Science and Technology, 10: 227

(Manuscript received 27 October 2011)
(Manuscript accepted 28 April 2012)
E-mail address of LEI Mingzhun: leimz@ipp.ac.cn